Seasonal Variation in Light Response of Polar Phytoplankton

T. M. Sloughter[a,*], N.S. Banas[a], R.N. Sambrotto[b]

[a] *Department of Mathematics & Statistics, University of Strathclyde*
[b] *Lamont-Doherty Earth Observatory, Columbia University*

Abstract

The seasonality of light response curves was observed in phytoplankton samples taken in the Eastern Bering Sea (EBS) shortly before and during the spring bloom. Under-ice samples were found to have lower values of both the maximum growth rate (μ_0) and the initial slope (α) of the photosynthesis-irradiance (PE) curve. This trend in α was also noted in a literature review of photoacclimation studies that looked at acclimation periods of 30 days or more. A trade-off is proposed between α and maintenance respiration such that below the compensation intensity E_C it becomes advantageous to decrease α to mitigate the costs of respiration. An existing NPZD model of the EBS was then extended to reflect this trade-off with a seasonal transition from low to high α, and likewise μ_0, at the point where available light is greater than E_C. A parameter analysis found that with this seasonal plasticity the model could accurately reproduce the timing and magnitude of the 2009 spring bloom using parameter combinations within realistic ranges. Without this seasonality, no parameter set could be found that reasonably reproduced the observations. This strongly suggests that ecosystem models of phytoplankton should consider the effects of seasonality within parameters, including α which may be lower in over-wintering populations.

*Corresponding author
Email address: trevor.sloughter@strath.ac.uk (T. M. Sloughter)

1. Introduction

Phytoplankton seasonality has long been understood to be an essential factor in temperate and high latitude marine ecosystems, with nearly a century of research acknowledging its fundamental importance (Gray, 1931) and attempting to understand the driving factors (Sverdrup, 1953). Evolutionary adaptations and individual acclimations to changes in temperature, nutrient concentration, turbulence, mixing depth, and light have all been scrutinised (Lichtman, 2000; Huisman et al., 2004), yet many of the mechanisms behind spring blooms and phytoplankton over-wintering strategies, especially as regards light response, remain not fully understood.

The light curves of phytoplankton, measures of growth or photosynthesis versus irradiance, are known to acclimate to changing light conditions (Sambrotto et al., 1986; Cullen, 1990; Lichtman, 2000) (see also references below). The initial slope of such a curve, denoted α, is often considered similar to a measure of photosynthetic efficiency.

The initial slope α, the maximum growth rate μ_0, and the saturation point E_k can all vary as phytoplankton respond to changing light through the processes photoacclimation, a plastic response within cells, photoadaptation, the evolutionary response within a population (Moore et al., 2006), or through an ecological shift in community composition. These processes may have significant impacts on timing and magnitude of spring blooms. For example, and as will be discussed in greater detail below, Banas et al. (2016b) found that a model hindcast of the Eastern Bering Sea required strong seasonal variation in α to reproduce detailed observations of bloom timing and magnitude simultaneously.

Responses to changes in light have been studied mostly on very short time scales. Many studies have explored how different phytoplankton respond to fluctuating light, on time scales as short as minutes (Strzepek and Harrison, 2004), hours (Fujiki and Taguchi, 2002; Ban et al., 2006), or days (Marra, 1978; Cosper, 1982; Nicklisch, 1998; Claustre et al., 2002). Typically, within these studies of short-term variation and acclimation the response observed has been

to increase photosynthetic efficiency as light diminishes, though there are exceptions (Sakshaug and Slagstad, 1991; Ban et al., 2006).

In contrast, Sambrotto et al. (1986) observed a rapid, nearly ten-fold increase in photosynthetic efficiency in the Southeastern Bering Sea during the onset of one spring bloom: the opposite of what simple photoacclimation would be expected to produce during a period of increasing light. Those results provided the motivation for imposing seasonality in α in the model of Banas et al. (2016b).

Seasonal change in photosynthetic efficiency necessarily reflects the net effect of a complex array of variable physiological processes. Changes in pigment concentration have a non-linear effect on efficiency. After a threshold is reached, excess pigments self-shade, creating what is known as the "package effect", reducing efficiency (Brunelle et al., 2012). Additionally, pigments require maintenance, and thus bear a metabolic cost in the form of maintenance respiration. Many cells have been shown to increase intracellular pigments as light decreases (Dubinsky and Stambler, 2009), but such trend can be the opposite after a period spent in zero light, after which pigments decrease again (Gibson, 1985). Peters and Thomas (1996) found that marine Antarctic diatoms preserved and maintained their photosynthetic apparati in winter and could resume assimilating carbon immediately upon the return of light after at least three months of darkness. In contrast, Peters (1996) observed decreased photosynthetic potential in temperate species, at higher temperatures, during long periods of darkness. This complexity, and variety of strategies, shows it is therefore difficult to create a unified theory of α seasonality.

This study builds on the above with more recent data from the Eastern Bering Sea which show lower values for both α and the maximum growth rate μ_0 in under-ice over-wintering samples compared with open-water samples in optimal spring bloom conditions. As noted in the following sub-section, this dormancy-like effect has in fact been reported repeatedly in the observational and experimental literature, although to our knowledge it has never previously been identified as a general high-latitude pattern.

Importantly, all the aforementioned adaptations and acclimations connect

photosynthetic efficiency with metabolism and respiration. In this study, we explore the idea that seasonal variations in photosynthetic parameters, particularly α, may be the result of seasonal energetic trade-offs, analogous to those that explain or predict winter dormancy in other taxa. A mechanistic theory is proposed that links α to respiration costs for polar diatom populations, and yields a simple numerical scheme that could be used to represent this physiology in oceanographic models. The case for lower α in over-wintering populations is further strengthened through a model case study of the Eastern Bering Sea.

1.1. Prior photoacclimation observations and experiments

A literature review (Tables 1 and 2) was conducted to establish whether the results of Sambrotto et al. (1986) and Banas et al. (2016b) in the EBS could likely be generalised. The literature on short term acclimation (from minutes to days) is vast and was sampled only to illustrate the variety. For long term acclimation, as we hypothesise a seasonal response, studies where samples of high-latitude phytoplankton which had 30 days or more to acclimate to light were specifically sought out. Decades of research into photoacclimation and photoadaptation have used a variety of methods and measured many different parameters. The papers surveyed here reflect the diversity of study methodology and phytoplankton strategy.

Tables 1 and 2 summarise the adaptations of α in response to decreases in light over time scales less than 30 days (Table 1) and longer than a month (Table 2), along with the impact of photoacclimation on chlorophyll-specific absorption $\bar{a}^*$. Photosynthetic efficiency α is a product of $\bar{a}^*$ and the maximum quantum yield $\phi_{\max}$:

$$\alpha = \bar{a}^* \phi_{\max} \tag{1}$$

As noted, in the Eastern Bering Sea, Sambrotto et al. (1986) found different values of α for pre-bloom and spring bloom samples taken in May 1981, with $\alpha_{summer} = 0.16$ (W m^{-2})$^{-1}$ day^{-1} and $\alpha_{winter} = 0.01$ (W m^{-2})$^{-1}$ day^{-1}.

In the units we use below, this corresponds to 3.0×10^{-2} (μE m^2 s^{-1})$^{-1}$ hr^{-1} (summer) and 1.9×10^{-3} (μE m^2 s^{-1})$^{-1}$ hr^{-1} (winter).

Previous literature demonstrates not only seasonal variability of photoparameters such as α and $\bar{a}^*$ but also variability in strategies (see Table 2). Two papers reporting α observations for marine phytoplankton over a seasonal time scale (Platt and Jassby, 1976; van Hilst and Smith, Jr, 2002) found lower values associated with a lower light regime. However another paper found the reverse trend for freshwater diatoms in a permanently ice-covered Antarctic lake (Morgan-Kiss et al., 2016). Sambrotto et al. (1986) compared light response between samples from Subsurface Chlorophyll Maximum (SCMs) and the overlying lower chlorophyll, higher light layers, and found larger α in the SCM. Palmer et al. (2011) found higher α in open water samples than in under-ice conditions in Franklin Bay but no significant difference in Darnley Bay. Palmer et al. (2013) also found no significant difference between open water and under ice in the Chukchi and Beaufort Seas. Rochet et al. (1986) found high variation in observed α from April to May, such that while the final measurement was lower than at the outset, the slight downward trend in the data was weak. Variation in $\bar{a}^*$ on a seasonal time scale was reported in Matsuoka et al. (2011), which found a decline in $\bar{a}^*$ going from spring to summer, Matsuoka et al. (2009) which found a slight increase between October and November, and Brunelle et al. (2012) which found a decrease from summer to autumn. A prior meta-analysis (Smith Jr. and Donaldson, 2015) of observations in the Ross Sea has also found photoparamters were sensitive to changes in irradiance.

Long term lab studies using cultures taken from field samples (Wulff et al., 2008), and experiments on lab cultures (Wu et al., 2008) also showed lowered α in lower light conditions. Though van Hilst and Smith, Jr (2002) found lower α in lower light in their field measurements, samples cultured in the lab and tested later with an acclimation period of 13 days had the reverse trend: higher α in lower light. Four studies looked at the response to decreasing light or total darkness (Wu et al., 2008; Wulff et al., 2008; Matsuoka et al., 2009; Morgan-Kiss et al., 2016), while three examined the response to an increase in light (Rochet

Source	Location	Taxonomy	Timescale	$\Delta\alpha$	μ_0	E_k	Notes
Short-Term Acclimations							
Ikeya et al. (2000)	44°N, Brackish Lagoon	*Chaetoceros* sp.	Hrs	$-^B$	$\sim$	+	
Sakshaug and Slagstad (1991)	$\sim$ 80°N, Barents Sea	*T. nordenskioeldii* & *C. furcellatus*	Days	$-^B$	–	–	Increase in ϕ_{max} at higher light, but decrease in a^*.
Ban et al. (2006)	Lab culture	*Chaetoceros gracilis*	Days	+		+	Comparing acclimation to 20 vs. 350μE m^2 s^{-1}. ETR correlated with light
				–		+	Comparing acclimation to 3 vs. 350μE m^2 s^{-1}. ETR correlated with light
van Hilst and Smith, Jr (2002)	76°36'S, Ross Sea	*Phaeocystis antarctica* and *Pseudonitzschia* sp. (lab cultures)	13 dys	$-^B$	$+^B$	+	

Table 1: Directional change of PE parameters acclimating to changes in light on short time scales (less than 30 days). A plus (+) indicates a higher value for the paramter was measured at the higher light level(s), a minus (–) indicates the reverse, and a $\sim$ indicates no significant difference. "B" indicates the study reported values of α^B, i.e. α normalised to biomass.

et al., 1986; van Hilst and Smith, Jr, 2002; Matsuoka et al., 2011; Brunelle et al., 2012).

The diverse observations on the interaction of phytoplankton light response with the seasonal physical oceanographic changes in temperate and polar regions is strong motivation for revisiting the interpretation of these parameters that are important to marine productivity. Here, we build on these field observations with an expanded, more recent dataset from the ice edge environment of the Eastern Bering Sea (EBS) along with a model representation of this phenomenon for a more mechanistic perspective.

Seasonal Acclimations							
Source	**Location**	**Taxonomy**	**Timescale**	$\Delta\alpha$	μ_0	E_k	**Notes**
Platt and Jassby (1976)	Costal Nova Scotia		Years: July '73 – March '75	$+^B$	$+^B$		
Sambrotto et al. (1986)	EBS	Diatom dominated (in spring)	Spring bloom transition	+	+		
This study	EBS	Centric diatom dominated (during bloom)	Under-ice vs. open-water; spring-bloom transition	+	+	~	
Rochet et al. (1986)	~ 55°30'S Hudson Bay	Diatom dominated (in May)	Months (March to May)	$\sim^B$	–		
van Hilst and Smith, Jr (2002)	76°30'S, Ross Sea	*Phaeocystis* dominated	Months (spring to summer)	$+^B$	$+^B$	–	
Wu et al. (2008)	Lab culture	*Microcystis aeruginosa* and *Scenedesmus quadricauda*	30 dys	+		+	ETR decreased at higher light
Wulff et al. (2008)	62°15'S	Diatoms, benthic (5-7 m depth)	64 dys	+		+	ETR increased at higher light
Palmer et al. (2011)	Darnley Bay Franklin Bay	Subsurface Chl Maximum	Open water vs. under-ice	~			
				$+^B$	$+^B$		
Palmer et al. (2013)	Chuckchi & Beaufort Seas	Community	Open water vs. under-ice	~	~	~	
Morgan-Kiss et al. (2016)	77°S, permanently ice-covered lake	Diatoms	31 Dys (Feb to March)	$-^B$	$+^B$	+	

Table 2: Directional change of PE parameters acclimating to changes in light on short time scales (less than 30 days). A plus (+) indicates a higher value for the paramter was measured at the higher light level(s), a minus (–) indicates the reverse, and a ~ indicates no significant difference. "B" indicates the study reported values of α^B, i.e. α normalised to biomass.

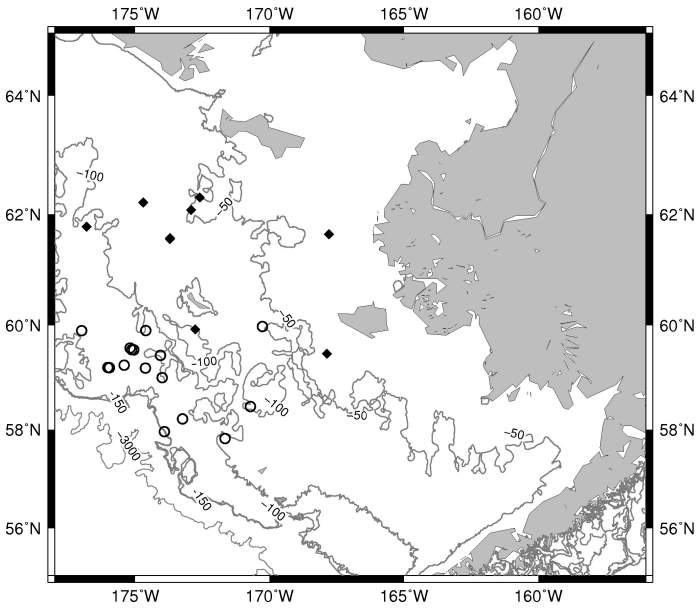

Figure 1: Location of the sample sites in the Eastern Bering Sea. Open circles represent open water sampling sites, and closed diamonds represent sites that were at least partially ice-covered at the time of sampling.

2. Methods

2.1. Cruise Data Analysis

Data were collected in the Eastern Bering Sea in spring 2007, 2008 and 2009 as part of the BEST-BSIERP field campaign on the USCG Healy (Sambrotto et al., 2015). The sample sites were in the mid- and outer shelf, with water depths ranging from 50 to 200 metres (Coachman, 1986).

The region experiences seasonal ice cover. Samples were collected before and after ice retreat during each cruise. Each vertical profile covered depths from the surface down to a light level of 1% of the surface value. A four-day-average light level $E_{above\,ice}$ was calculated by measuring incident light on the deck of the ship on the day of sampling and the three days prior.

Uptake rates of NO_3 and inorganic C were measured in the same incubation bottle using a dual-label approach with a combination of the stable isotope tracers $^{15}NO_3$ and $H^{13}CO_3$ (Sambrotto, 2001; Sambrotto et al., 2008). Samples

were taken from the euphotic zone (100, 55, 30, 17, 9, 5 and 1.5% of maximum submarine light) and collected in 2.2-L PET bottles. The original light levels were simulated with layers of black screen and the bottles were incubated for 24 hours in on-deck incubators cooled with surface seawater pumped from the ships sea chest. Complete details of sampling and measurement procedures can be found in Sambrotto et al. (2015).

The photoparameters (here denoted μ_0, α, E_k, and β) were derived fitting the carbon uptake data with the Platt model (Platt et al., 1982):

$$\mu = \mu_0 \left(1 - \mathrm{e}^{-E/E_k}\right) \mathrm{e}^{-\beta E/\mu_0} \tag{2}$$

Here, μ_0 is the maximum growth rate (referred to as $P_{\max}$ in Sambrotto et al. 2015), E_k is the saturation light intensity, and β is the photoinhibition parameter. The parameter α, the initial slope of the PE curve, often referred to as photosynthetic efficiency, is defined in this formulation as

$$\alpha = \frac{\mu_0}{E_k} \tag{3}$$

Though β was fit with the other parameters, it only impacts the Platt Model at higher light levels than were relevant to the present study. Therefore, in the theoretical discussions below regarding the Platt model and photoacclimation, the β component of the equations is ignored for the sake of clarity. A more realistic version would include photoinhibition, but the overall trends would be the same.

Measured values of μ_0 , α, and E_k are shown in Fig. 3 as a function of the light at the water surface surface, E_{surf}. As mentioned, a three-day average irradiance was measured from the deck of the ship and taken as the above-ice light level. Under ice light values had to be corrected for attenuation by the sea ice. This attenutation is highly dependent on factors which were not measured, including ice thickness, density of ice algae, and snow thickness (Kauko et al., 2017).

The value of E_{surf} below the ice was estimated as a linear function of the deckboard-measured light and percent ice cover C, as without more data a more complicated model of attenuation could not be justified. The linear form used here was fit such that in areas with complete ice cover, it was assumed that no light reached the water surface:

$$E_{surf} = E_{above\,ice}\left(1 - \frac{C}{100}\right) \tag{4}$$

The assumption of there being no trasmittance at maximnum ice cover is reflective of observations and studies showing that ice and snow cover in winter can dramatically decrease transmittance (Assmy et al., 2017; Kauko et al., 2017). The possibility and implications of this approach under-estimating light transmittance is discussed in the results below.

2.2. Model of Maintenance Respiration

As noted by Platt and Jassby (1976), the commonly used form of the Platt curve represents gross growth rate, not net. Gross growth is the sum of net growth and dark respiration R_D. Thus, Cullen (1990) rewrote the Platt Model to explicitly include respiration by taking growth μ in Equation 2 to be the gross growth rate:

$$\mu_{net} + R_D = \mu_0\left(1 - \mathrm{e}^{-\alpha E/\mu_0}\right) \tag{5}$$

It has been show that dark respiration is a linear function of growth rate μ (Falkowski and Raven, 2007), such that

$$R_D = r\mu_{gross} + R_M \tag{6}$$

where r is a species-specific slope, and R_M is maintenance respiration which occurs even when there is no growth.

Combining Equations 6 and 5 and solving for μ gives

$$\mu = (1 - r)\,\mu_0\left(1 - \mathrm{e}^{-\alpha E/\mu_0}\right) - R_M \tag{7}$$

Assuming $r \ll 1$, as is common in plankton models, the resulting equation is the original Platt model minus maintenance respiration.

Following Langdon (1988), maintenance respiration can be expressed as a product of α and the compensation intensity E_C, i.e. the light level at which respiration and gross growth rates balance and net growth is zero.

$$R_M = \alpha E_C \tag{8}$$

This relation expresses the idea that an increase in α necessitates an increase in photosynthetic machinery and thus a higher energy cost to maintain, which has been shown empirically to approximately follow the linear relation shown above (Langdon, 1988). Inserting this formulation into equation 7 gives:

$$\mu = \mu_0 \left(1 - \mathrm{e}^{-\alpha E/\mu_0}\right) - \alpha E_C \tag{9}$$

Based on EBS observations (see Results below), the variation in E_k appears to be weakly correlated with seasonal changes, if at all. But μ_0 does correlate with α, and exhibits the same seasonal pattern. Thus if we assume E_k is not seasonal, then it can be taken as constant with respect to time, or with respect to seasonal parameters, e.g. $\partial E_k/\partial\alpha = 0$. And since $\mu_0 = \alpha E_k$, then $\partial\mu_0/\partial\alpha = E_k$. Under this assumption the dependence of net growth on α becomes

$$\frac{\partial\mu}{\partial\alpha} = E_k \left(1 - \mathrm{e}^{-E/E_k}\right) - E_C \tag{10}$$

In conditions where $\partial\mu/\partial\alpha > 0$, increased photosynthetic efficiency leads to an increase in net growth as expected, but where $\partial\mu/\partial\alpha < 0$, decreasing α becomes energetically beneficial. The threshold light level, E_*, which marks the boundary between these regimes is that which makes $\partial\mu/\partial\alpha$ equal to zero,

$$E = E_* \equiv E_k \ln\left(\frac{E_k}{E_k - E_C}\right) \tag{11}$$

The Taylor expansion for $E_*(E_C)$ around $E_C = 0$ is:

$$\begin{aligned} E_* &\approx E_*(0) + E_k \frac{\partial}{\partial E_C} \left[\ln \frac{E_k}{E_k - E_C} \right] \cdot E_C + \mathcal{O}(E_C^2) \\ &= 0 + E_k \frac{1}{E_k} E_C + \mathcal{O}(E_C^2) \end{aligned} \tag{12}$$

where $\mathcal{O}(E_C^2)$ denotes terms of the second and higher orders. These terms are increasingly vanishingly small for small values of E_C, and can be ignored.

The first order approximation (ignoring the errors of higher order) yields

$$E_* \approx E_C \tag{13}$$

for small values of E_C. This is to be expected, given the Platt Model's linearity at low irradiances.

Below the compensation intensity, respiration is greater than growth and can be minimised by decreasing α. It is expected then when the light experienced by the community increases above E_C, the balance should shift from low to high α.

2.3. NPZD Model

An existing NPZD model hindcast, developed for the East Bering Sea (Banas et al., 2016b), was modified into two versions: a model with seasonality in μ_0 and α and a model without seasonality (i.e. constant photoparamters throughout the year). The components of the model are shown in Fig. 2. The model has a six-compartment nitrogen budget and tracks phytoplankton biomass P, microzooplankton biomass Z, small and large detritus, and the nutrients NO_3 and NH_4. Phytoplankton growth μ is a function of irradiance and concentration of NO_3 and NH_4, with loss terms from microzooplankton ingestion I, mortality m_P and aggregation m_{agg}.

Physical forcing was taken from the BESTMAS (Bering Ecosystem Study ico-ocean Modeling and Assimilation System) model, described and validated in Zhang et al. (2010). The NPZD model is one-dimensional, but is able to

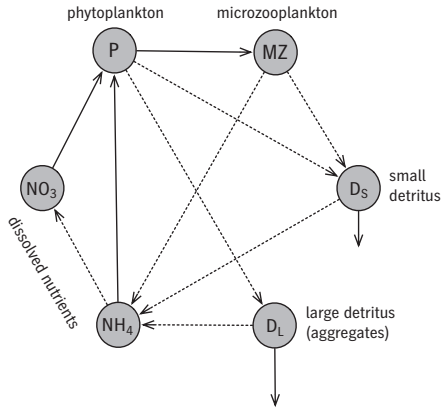

Figure 2: Structure of the ecosystem model, reproduced from Fig. 4 in Banas et al. (2016b). Solid arrows denote growth for the compartments being fed into, with the exception of the solid arrows from detritus which are losses from the system. Dotted arrows denote regeneration pathways.

capture advection as a flow-following water column. Physical forcing was extracted from BESTMAS along particle trajectories which follow the 0–35 m depth-average currents and which intersect with the region of interest in time and space.

The equation of phytoplankton growth in the NPZD model accounted for total nutrient concentration (N_{tot}, with a saturation constant k_{min}) as well as light:

$$\mu = \left(\frac{\alpha E}{\sqrt{\alpha^2 E^2 + \mu_0^2}} \right) \left(\frac{N_{tot}}{k_{min} + 2\sqrt{k_{min} N_{tot}} + N_{tot}} \right) \mu_0 \tag{14}$$

The amount of light experienced by a cell in the water column was defined with respect to light at the water surface E_0, attenuation by sea-water att_{sw}, and the ratio of vertical diffusivity κ to the doubling time of cells μ_0:

$$E_{eff} = E_0 \exp\left(-\mathrm{att}_{sw} \sqrt{\frac{\max\kappa}{\mu_0}} \right) \tag{15}$$

In the case of the model with seasonal photoparameters, once E_{eff} exceeded the compensation intensity E_C, winter values for α and μ_0 switched to higher summer values. For both parameters, the transition was defined by a hyperbolic

tangent function:

$$\alpha = \alpha_{win} + \frac{1}{2}\left(\alpha_{sum} - \alpha_{win}\right)\left(1 + \tanh\frac{E_{eff} - E_C}{\Delta E}\right) \tag{16}$$

There was no such change for the model version without seasonality, the only difference between these two variations of the model was the absence of the above equation and the use of constant α and μ_0 for the nonseasonal model.

The tuning of these model versions was done through a Monte Carlo process, varying the model parameters in 200 000 different runs. These runs were then compared with observational data taken in spring and summer 2009 in the mid-shelf region of the EBS, referred to here and in the prior paper as the "IEB60" case.

The IEB60 data resolved an ice-edge spring bloom near 60°N in late April to early May, 2009, from BEST/BSIERP observations (Lomas et al., 2012; Mordy et al., 2012; Stabeno et al., 2012; Stoecker et al., 2013; Sherr et al., 2013; Sambrotto et al., 2016). These included concentrations of NO_3, phytoplankton and microzooplankton biomass, growth rates determined from dilutions as well as ^{14}C, ^{13}C, and ^{15}N uptake experiments.

In the prior paper, the model already contained seasonality in α that was enabled by an arbitrary critical light level. When the effective light, E_{eff} experienced by a phytoplankton cell in the mixed layer exceeded this critical light level, the model switched from low pre-bloom winter α to a high summer α. This transition was defined by a hyperbolic tangent function. Here this critical light level is replaced by the compensation light intensity E_C. As the model was nitrogen based and not carbon, the maintenance respiration cost in Equation 9 was not explicitly defined.

The parameter analysis was conducted with respect to ten parameters (shown in Table 3). These parameters were selected on the basis of observational uncertainty (i.e. there was justification for considerable flexibility in their values) and their relevance to the new model (i.e. α and μ would necessarily need retuning in a model that arguing for their change, as would related terms such as E_C).

Nine of the parameters were randomly varied over the course of 50 000 model runs. In each run, each of these parameters was assigned a random value from a wide range that encompassed prior observations. This range was a factor of 3 above and below the parameters used in Banas et al. (2016b). The exception was for E_C, whos range was from 0 to 25 W m^{-2}, a rough estimate based on prior literature (Quigg and Beardall, 2003; Langdon, 1988).

Effectively, this was a brute-force approach to searching a broad parameter space for possible good fits. Because it was assumed that E_k was constant, once α_{sum} and $\mu_{0,sum}$ were selected, E_k was fixed. As a result, the tenth parameter, α_{win} was fixed by the selection of $\mu_{0,win}$, as a result of

$$\alpha_{win} = \mu_{0,win}\frac{1}{E_k} = \mu_{0,win}\frac{\alpha_{sum}}{\mu_{0,sum}} \tag{17}$$

The results of each run were also compared with the IEB60 data: NO_3 concentrations, phytoplankton and microzooplankton biomass (P and Z), f-ratio, and the growth μ and grazing rates I of phytoplankton and microzooplankton, respectively.

A cost c was then calculated from the mean-squared error between the model outputs m_i and the observed data points o_i.

$$c = \frac{1}{n}\sum_i \left(\frac{o_i - m_i}{\sigma_i}\right)^2 \tag{18}$$

The values of o_i correspond to averages of each metric (e.g. NO_3 concentration) at a specific phase in bloom development. The four phases considered were pre-bloom, early bloom, late bloom, and summer. For each metric, an average was taken of the observational data and the model outputs within each of the four phases, producing four points for each metric representing different periods in time. This averaging was done to eliminate potential sampling bias that might give more weight to one time period over the others.

The term σ_i reflected a heuristically determined range of error for each metric, such that the model was not constrained to get as close as possible to the

actual points, but within a wide range.

The parameter combinations which yielded model runs that minimised c for the model without seasonality were compared with those for the model with seasonality. As this was a random sampling without direction, there was no cutoff or target value for c, both the seasonal and nonseasonal models were given 50 000 runs each in the tuning process. The lowest cost results were then compared for their ability to capture key observations such as the timing and magnitude of the phytoplankton bloom and the corresponding rapid decrease in NO_3 concentration.

3. Results

3.1. Cruise Data

Fig. 3 shows observed values of the three relevant PE parameters μ_0, α, and E_k plotted against PAR at the water surface (E_{surf} as defined in Eq 4). In Fig. 3b, two clusters appear in the data for α. Open water samples have a mean $\alpha = (3.1 \pm 1.3) \times 10^{-4}$ (μE m^2 s^{-1})$^{-1}$hr^{-1}. In under ice samples, values of α are generally lower than in open water populations, with a mean of $\alpha = (1.3 \pm 2.0) \times 10^{-4}$ (μE m^2 s^{-1})$^{-1}$hr^{-1}.

One outlier stands out in the under ice samples shown in Fig. 3b, at $E_{surf} = 43.2$ μE m^2 s^{-1}. Given the complex wind-driven transport of sea ice in the area, it is possible that this or other samples taken from locations identified as ice-covered may have previously been in open water, such that their phytoplankton could have already acclimated to open-water conditions and higher light levels. This is only a speculation regarding this particular outlier, but we note that without it, the under-ice values of α have a mean of $(0.65 \pm 0.4) \times 10^{-4}$ (μE m^2 s^{-1})$^{-1}$hr^{-1}.

A one-tailed Mann-Whitney U test was conducted to establish the significance of the observed difference. Including the outlier in the under-ice data, $U_{under\,ice} = 17$ and $U_{open\,water} = 111$, indicating that the under-ice values are significantly lower than open water ($p < 0.01$). The same pattern is found

even when normalised to chlorophyll, that is $\alpha^B = \alpha \frac{\mathrm{C}}{\mathrm{Chl}}$. Here, a one-tailed Mann-Whitney U test also shows statistical significance for the hypothesis that $\alpha^B_{under\,ice}$ is less than $\alpha^B_{open\,water}$ ($\mathrm{p} < 0.05$).

A similar but less dramatic pattern appears in the data for μ_0. The mean for under-ice values was 0.014 ± 0.016 hr^{-1}, while open water samples, $\mu_{0,\mathrm{avg}} = 0.026 \pm 0.015$ hr^{-1}. The difference is also significant ($\mathrm{p} < 0.05$) by a one-tailed Mann-Whitney U test where, including the outlier, $U_{under\,ice} = 31$. Values of E_k do not appear to differ significantly between under-ice and open-water conditions. For under-ice samples, $E_k = 120 \pm 60$ μE m^2 s^{-1}. Open-water samples had $E_k = 100 \pm 80$ μE m^2 s^{-1}.

3.2. Trade-off

The impact of seasonal α is demonstrated in Fig. 4, which shows the extended Platt Model (given in Equation 9) for the two mean values of α reported above, and using a hypothetical value of E_C.

As demonstrated in Section 2.2 and shown in Figs 3 and 5, the compensation intensity E_C is the threshold below which it is more advantageous to have a decreased α and thereby decrease losses due to respiration. Therefore by estimating E_C and comparing with the observed transition light level, the model can be tested for consistency with the Eastern Bering Sea data.

This required establishing the mean PAR experienced by the sampled phytoplankton, a function of mixing depth, turbulence, surface PAR, and ice cover. In the mixed layer, individual cells move up and down from the surface to near darkness, and the average light experienced by one cell is significantly less than the maximum. With insufficient data to establish more realistic estimates, mean PAR was approximated by applying a single correction factor to the surface PAR, such that $E_{mean} = cE_{surf}$.

This correction factor c was estimated to be 0.2, based on observations in environments with similar mixed-layer depths (Diehl et al., 2002; Long, 2010). This approximation also matches the biophysical model of Banas et al. (2016b, cf. Fig. 7 in that study), and corresponds to uniform mixing of a 40 m euphotic

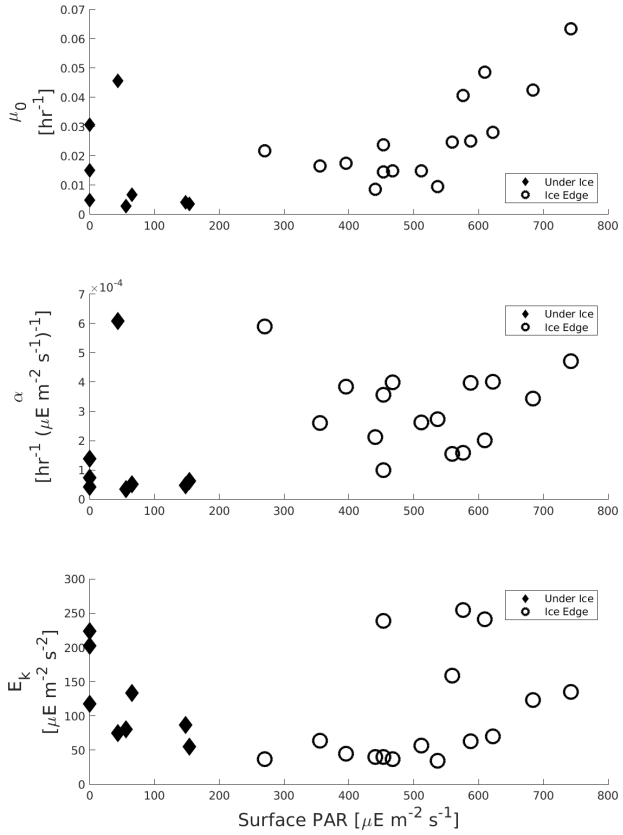

Figure 3: Photoparameters plotted against surface PAR. Open circles are data from open-water sampling sites, closed diamonds are data from sites that were at least partially ice-covered at the time of sampling.

zone.

The cruise data is replotted in Fig. 5 as a function of this estimated E_{mean} as opposed to E_{surf}. A range for E_C estimated from the literature (5–25 μE m^2 s^{-1}: cf. Quigg and Beardall (2003); Langdon (1988)), as well as the corresponding range of E_* values, lie across the domain between total darkness and spring-bloom light levels. As mentioned in Section 2, the actual transmittance through the ice was not known. Higher transmittance would shift all the under-

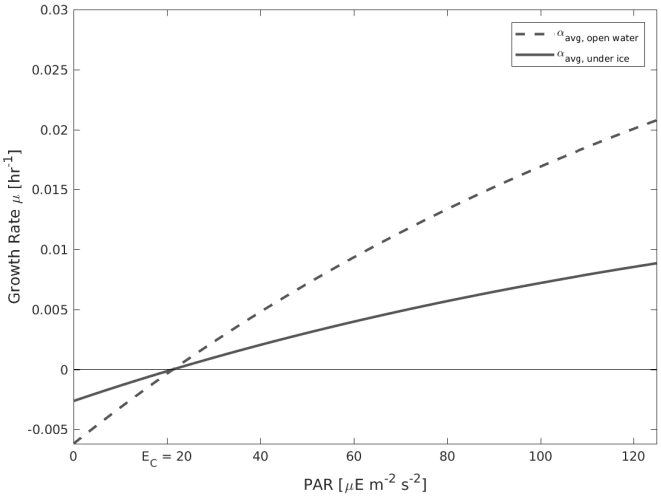

Figure 4: Hypothetical growth curves given by the model given in Equation 9 using the mean values of observed α for open water and under-ice samples and the average μ_0 for open-water samples (see Fig. 3 and Section 3.1). As E_k was assumed to be constant, its value was calculated from the open water values of μ_0 and α, and the result was used to calculate μ_0 for the under ice curve based on Equation 3. Above the compensation point (here arbitrarily chosen to be $E_C = 20$ μE m^2 s^{-1}), larger α is clearly advantageous, however below this point respiratory losses dominate and a lower α leads to lower loss.

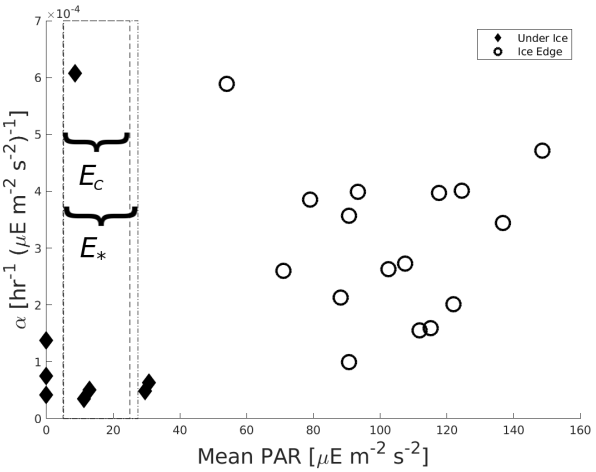

Figure 5: Observed α plotted against the approximate mean PAR cells would experience in the mixed layer. See Fig. 3b for the plot of α against surface PAR. The rectangular boxes indicate the estimated range of E_C and subsequent range of E_* using Equation 12 and the mean values of E_k (see Section 3.1). As was shown in Equation 13, E_* deviates only very slightly from E_C, the offset being negligible when $E_k \gg E_C$.

ice points toward higher PAR in the figure. Two points are already outside the potential domain of E_C, though even one third of the light penetrating the snow, ice, and ice-algae would still result in the majority of under-ice points within this domain.

The EBS data are thus consistent with the energetic model above, or rather, as consistent as we might expect them to be given the uncertainty surrounding the exact light environment and light history of the sampled plankton patches.

3.3. NPZD Modelling

The best fit model runs with the lowest costs c are show in Fig. 6, plotted with the observational data. While noticeable errors still remain at specific points, the model run with seasonality performs substantially better.

The IEB60 data show nitrate declining rapidly as phytoplankton biomass and growth rates increase. It should be noted in July many measurements recorded an increase in NO_3. One source of this error could be a pycnocline shallower than 35 m, with the high concentration mostly being below the py-

cnocline but increasing the 0–35 m depth average. It may also be the result of the limits of the one-dimensional approach used here, as it does not fully reproduce patchy wind mixing, which may be a source of intermittent resupply of nitrate (Eisner et al., 2016).

Without seasonality, the best fit runs were unable to reproduce the magnitude of the spring bloom in terms of phytoplankton biomass. As can be seen in Fig. 6, there is a slight increase in P biomass around the corect date, but is an order of magnitude below the observed peak. More importantly, even if the magnitude is increased through an increase in α or μ_0, a spurious early bloom becomes increasingly pronounced. When the other observational metrics are ignored and only the error for P biomass is examined, the magnitude of the bloom can be replicated but also occurs a month or more too early.

With seasonality, however, stronger fits are found. While the lowest cost for the nonseasonal model was $c_{min,nonseasonal} \approx 1.771$, the model with seasonality was able to reduce the minimum cost by over a third, with $c_{min,seasonal} \approx 0.496$, and no spurious bloom. Many low cost ($c < 0.7$) fits for the seasonal model still have spurious early blooms, however, and these are shown in Fig. 6 for completeness.

Caveats for the success of the model include that the highest values of error exist for the microzooplankton grazing rates and biomass. The parameter ranges for these fits are shown in Table 3. E_C remains the most uncertain parameter, as there is limited data for comparison.

4. Discussion

As demonstrated above, distinguishing seasonal variation in α from short-term variation is important to understanding the strategies of high-latitude phytoplankton. Short-term variation can be brief, and frequently changes in α occur in the opposite direction than on seasonal scales. These distinction means the impacts of photoacclimation on long time scales may be counter-intuitive.

The data presented here and in the literature cited attest to this. Although the data presented from the 2007-2009 cruised were sampled in different regions at similar times of year, there are good reasons to believe they represent seasonal change. Spatially, the under-ice and open water regions were not very distinct, with surface currents exchanging water between them (Stabeno et al., 2016). Additionally, prior obserations of this seasonality in the EBS (Sambrotto et al., 1986) and elsewhere (see Tables 1 and 2) have been more explicitly seasonal in their time scales.

However, in the simple form of the Platt Model, all other parameters being equal, a greater value of α leads to higher rates of photosynthesis and growth. This model alone does not predict why over-wintering cells would decrease α. Expressing α in terms of a respiration cost (Equation 8) provides such an explanation.

The EBS ecosystem model of Banas et al. (2016b) fit a transition from low winter α to high summer α at a threshold light level in an ad-hoc way by tuning to observations. In contrast, the model in Equation 9 predicts a threshold light level *a priori*. The nature of this transition, whether it is abrupt or gradual, is yet uncertain, and more data is needed from this range to clarify, however it was still possible to generalise the trend in the model. The results of the model analysis strongly suggest that such seasonality is necessary to fully explain bloom dynamics in the EBS.

4.1. Physiology

There are many factors which can lead to a decrease in α. In the case of over-wintering in polar ecosystems, the need for efficiency in low light regimes must

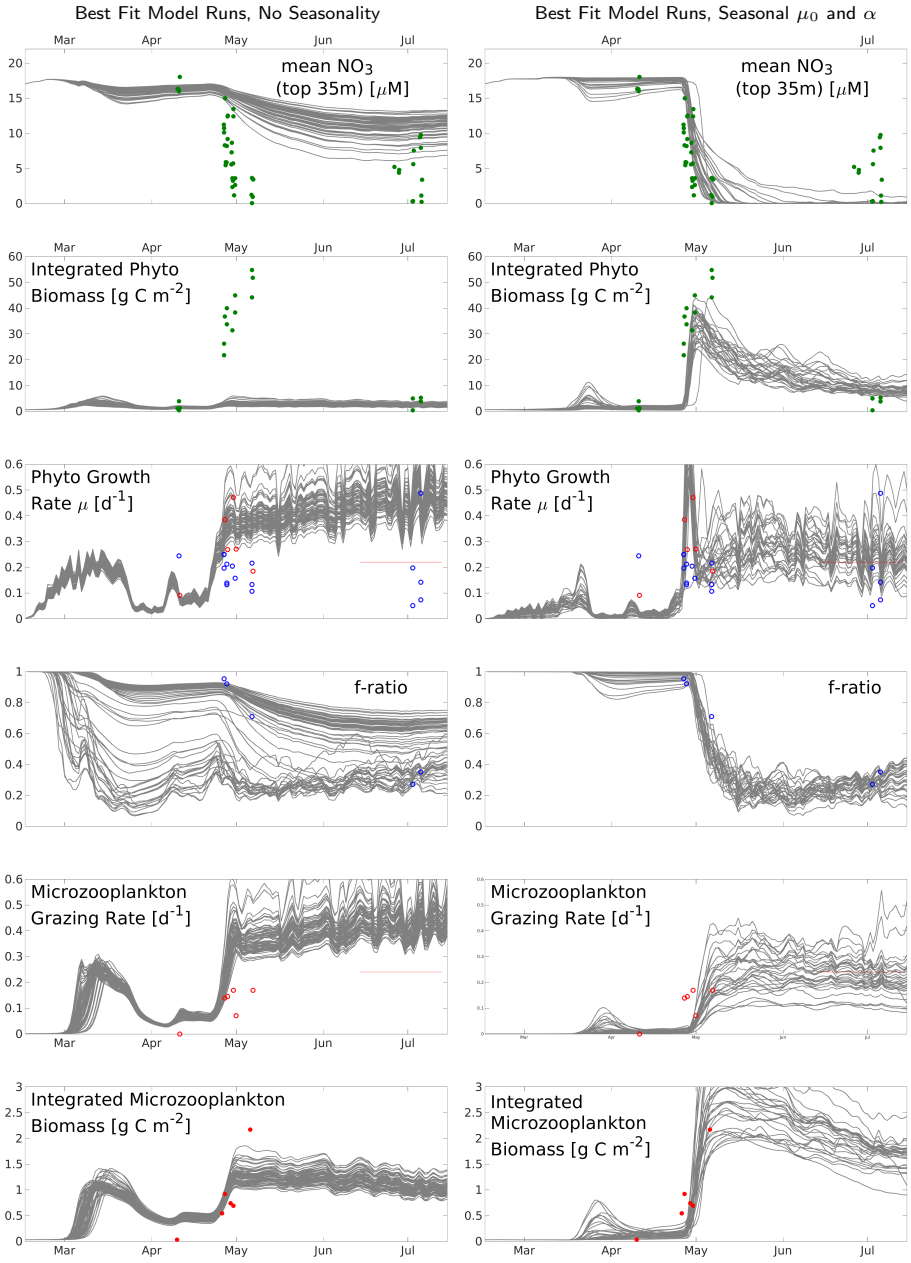

Figure 6: The best fitting model results, as determined by the cost function using observational data, for the NPZD model without seasonal photoparameters (left column) and the NPZD model with seasonal α and μ_0.

be balanced with the respiratory costs of maintaining photosynthetic apparati. The association of α with R_M in Langdon (1988) was derived from a fit to experimental data, yet the physical underpinning of this relationship can be seen in Equation 1, expressing α as a function of chlorophyll-specific absorption cross-section $\bar{a}^*$ and maximum quantum yield ϕ_{max}.

Chlorophyll-specific absorption cross-section $\bar{a}^*$ is a measure of the amount of PAR absorbed by chlorophyll-a, normalised to the amount of chlorophyll-a. Increases in chlorophyll-a arranged in a thin layer or shell increase the amount of surface area to absorb light and therefore cause an increase in $\bar{a}^*$. Excessive pigment depletion can lower the absorption cross section, thereby reducing α (Dubinsky and Stambler, 2009). However, in a three-dimensional cell, chlorophyll can self-shade. This self-shading is known as the "package effect", and it causes an effective decrease in absorption cross section while increasing the total amount of chlorophyll-a, causing a decrease in $\bar{a}^*$ (Rochet et al., 1986). Thus either an increase or decrease in chlorophyll can cause a decrease in $\bar{a}^*$ and therefore α, generally speaking. Both phenomena have been observed in polar phytoplankton (Jochem, 1999).

Another layer of complexity is added by the diversity of pigments. While $\bar{a}^*$ may decrease as a result of decreased chlorophyll, an increase in other pigments mean the cell may still darken and the overall absorption remain the same or even increase (Matsuoka et al., 2009, 2011). In that sense, $\bar{a}^*$ is not always a proxy for α, and the whole photosystem must be considered, a helpful parameter being ϕ_{max}.

Maximum quantum yield ϕ_{max} can be defined as the ratio of the absorption cross sections of Photosystem II (PSII) and the Photosynthetic Unit (PSU).

$$\phi_{max} = \frac{\sigma_{\mathrm{PSII}}}{\sigma_{\mathrm{PSU}}} \tag{19}$$

The photosynthetic unit is not, strictly speaking, a physical element, but a representation of the whole system of processes from absorption of a photon to production of O_2. The "size" of the PSU can be represented as the ratio of

chlorophyll to evolved oxygen (Chl/O_2) (Falkowski and Raven, 2007). The PSU accounts for the antennae and reaction centres of a photosystem, as well as the chlorophyll which carries electrons between them.

Thus the maintenance respiration cost associated with α could be the effect of any of several of the molecular mechanisms of photosynthesis: the amount of chlorophyll-a, or the amount of reaction centres or other pigments in the antennae. Chlorophyll concentration needn't necessarily decrease for α to decrease either, as the package effect yields a reduction in $\bar{a}^*$. Many diatoms are known to increase their pigments and darken as light decreases (Dubinsky and Stambler, 2009).

Moreover, adding to the complexity is the fact that antennae and reaction centres can be regulated independently (Falkowski and Raven, 2007). Decreasing reaction centres increases the "size" of the PSU by decreasing the amount of evolved O_2 per amount of chlorophyll, effectively increasing σ_{PSU} and therefore decreasing ϕ_{max} while saving respiration costs. Morgan-Kiss et al. (2016) describe possible processes of down-regulating this activity in freshwater Antarctic communities. The implication of these multiple regulatory processes is that the hypotheses of this paper may bee too simple to fully explain the high degree of variation that is noted in the literature on a purely mechanistic basis. But in spite of these complications, a large scale trend does appear to follow through as evidenced in the model experiments.

4.2. Taxonomy

It should be noted that neither these considerations nor the results of our literature review (Tables 1 and 2) suggest a simple hypothesis regarding the taxonomic scope of the strategy of winter reduction in photosynthetic efficiency. Further, a question remains whether the variation in PE parameters for a whole community represent intra-cellular photoacclimation, or a shift in community composition.

Matsuoka et al. (2011) propose changes in community composition from larger to smaller cells as the driving factor in decreases in $\bar{a}^*$, as the package

effect decreases with cell size. Decreases in α may be explicable as the result of decreased $\bar{a}^*$ in regions where spring blooms are dominated by diatoms with larger cell sizes than winter communities, such as the EBS in this paper and Sambrotto et al. (1986, 2015), the Ross Sea in van Hilst and Smith, Jr (2002), or the Amundsen Gulf in Palmer et al. (2011, 2013).

As for whether specific taxa have common strategies of photoacclimation, Jochem (1999) distinguishes two types of long-term dark response in global phytoplankton: those which decrease metabolic activity (Type I) and those which do not (Type II). Type II populations require a period of replenishing when re-illumination begins before cells can divide again. The same study found three subjects (*Brachiomonas submarina*, *Pavlova lutheri*, *Chrysochromulina hirta*) to be Type I and three more (*Prymnesium parvum*, *Bacteriastrum* sp. and an unidentified pennate) to be Type II.

Spring blooms in the EBS are dominated by centric diatoms (Sambrotto et al., 2015), and our study has found that community to be Type I, in the terms of Jochem (1999). In contrast, Peters and Thomas (1996) reported that several marine polar diatoms maintain their photosynthetic apparati in winter, as indicated by rapid growth responses upon re-illumination and measures of Chl-a. (It should be noted the darkness in that study lasted only to a maximum of 12 days). Still, Peters and Thomas (1996), Jochem (1999), and Dubinsky and Stambler (2009) all cite literature attesting to other diatom species which decrease metabolism over winter, suggesting a blanket strategy based on taxonomy may not be possible to formulate.

4.3. Implications for Model Design

In the previous study (Banas et al., 2016b), it was established that seasonality in α needed to be accounted for to reproduce observed data. This paper has provided evidence that this seasonality can be seen in the data gathered from Bering Sea communities (as well as other high-latitude environments, cf. Table 2). That this model performs well when considering seasonality in both α and μ_0, and cannot accurately reflect the data without seasonality, fits well with the

observation of seasonality shown in the data above.

While many ecosystem models do not account for seasonality in these parameters, we have provided evience that such seasonality may well be essential for accuracy of bloom timing and magnitude. We have also provided a simple mechanistic explanation and a means of implementing seasonality with minimal alterations to the model.

Questions of interpretation still remain, however. Many of the studies cited in this paper not only demonstrate changes in community composition during spring blooms, but also measured α on a community level and not separately by species (see Table 2).

Photoparameters can also be affected by nutrient limitation (Smith Jr. and Donaldson, 2015). In these experiments, nutrient limitation was not relevant until the bloom was fully initiated. The focus of these experiments was on the run-up to the spring bloom and the timing of its onset, all periods where in the model nutrients were saturated. In other scenarios or models this may not be the case, and could be a confounding factor.

Considering further the possibility that the better fitting of the seasonal model is more to do with extra degrees of freedom, the model used here is also a 1-P case. It is possible that with 2 phytoplankton classes, or more, that for each class smaller variations in α or even none at all are sufficient to provide a good fit to data, if the classes with higher α become dominant in spring.

Yet the literature review still shows individual cells can experience seasonal α, making this a necessary consideration for modelling efforts even with multiple phytoplankton classes.

The pressing implication for model design from this study is the sensitivity of the spring bloom to seasonality of light response. While numerous complicated factors have been expounded upon above, and new degrees of freedom increase flexibility generally, the fundamental change of the model from a static light response to one which can in a very short time switch from slow to rapid growth fundamentally enables a rapid bloom. Importantly, while the rapid bloom can be captured with the nonseasonal model, the threshold light level used in the

seasonal model allows for a tuning of the timing of the bloom, making it significantly easier to match both timing and magnitude together.

5. Conclusion

In summary, samples of phytoplankton in the Eastern Bering Sea taken from sea-ice-covered locations have markedly smaller values of α than do those taken in open water sites at the onset of the spring bloom. This pattern is consistent with previous literature on photoacclimation on timescales of months or more, including previous observations and modelling of the Eastern Bering Sea.

A mechanistic explanation which relates α to maintenance respiration and thus quantifies the trade-off between photosynthetic efficiency and energy expenditure predicts a transition light level, close to the compensation light level E_C, below which reduction in α is predicted to be the optimal seasonal strategy. This theoretical result is consistent with EBS observations.

Furthermore, the sensitivity of an NPZD model to seasonality in α and μ_0 strongly suggests the importance of this process (or these processes) on phenology and magnitude of the spring bloom. Whether this can better be explained as a change in community structure, with a population that naturally have higher α increasing in fraction from spring to summer, is yet to be fully answered.

A 1-P model must still reflect the overall changes in α, however, whether it is representing community shifts or intracellular change (though the above has shown both processes are likely to be relevant). Future projects with these models and paradigms will explore the abilities of a 2-P model. Comparisons of 2-P and 1-P variations will help differentiate between improvements due merely to extra degrees of freedom as opposed to improvements that reflect fundamental processes.

In a warming world, Arctic regions will experience drastic environmental changes. As temperatures rise and ice retreats, the seasonal patterns and adaptive strategies of polar phytoplankton will change as well (Matsuoka et al., 2009). Acknowledging the complexities and often counter-intuitiveness of their

seasonal behaviour is essential for accurately predicting these developments. Seasonal strategies are already a central component of models of mesozooplankton and higher trophic levels in high latitudes (Varpe et al., 2007; Ji et al., 2012; Banas et al., 2016a), and our results suggest that this approach might well need to be extended to phytoplankton as well. The simple physiological model developed above provides a means of incorporating dormancy-like dynamics into standard phytoplankton growth models. Observations and experiments that can test the generality of our results across polar regions and phytoplankton taxa, and provide insight into the specifics of the winter-to-spring transition, are badly needed.

6. Acknowledgements

Many thanks to Juan Bonachela, Laura Hobbs, Sofia Ferreira, Mike Heath, Dave McKee, and Geir Johnsen for helpful discussions.

7. Funding

This work was supported by grants to University of Strathclyde from Marine Alliance for Science and Technology Scotland (MASTS) and the Natural Environment Research Council (NERC) Changing Arctic Ocean programme.

8. References

Assmy, P., Fernández-Méndez, M., Duarte, P., Meyer, A., Randelhoff, A., Mundy, C. J., Olsen, L. M., Kauko, H. M., et al., A. B., 2017. Leads in arctic pack ice enable early phytoplankton blooms below snow-covered sea ice. Sci Rep 7 (40850).

Ban, A., Aikawa, S., Hattori, H., Sasaki, H., Sampei, M., Kudoh, S., Fukuchi, M., Satoh, K., Kashino, Y., 2006. Comparative analysis of photosynthetic properties in ice algae and phytoplankton inhabiting franklin bay, the canadian arctic, with those in mesophilic diatoms during cases 03-04. Polar Bioscience 19, 11–28.

Banas, N. S., Møller, E. F., Nielsen, T. G., Eisner, L. B., 2016a. Copepod life strategy and population viability in response to prey timing and temperature: Testing a new model across latitude, time, and the size spectrum. Frontiers in Marine Science 3 (225).

Banas, N. S., Zhang, J., Campbell, R. G., Sambrotto, R. N., Lomas, M. W., Sherr, E., Sherr, B., Ashjian, C., Stoecker, D., Lessard, E. J., 2016b. Spring plankton dynamics in the eastern bering sea, 1971–2050: Mechanisms of inter-annual variability diagnosed with a numerical model. Journal of Geophysical Research: Oceans 121 (2).

Brunelle, C. B., Larouche, P., Gosselin, M., 2012. Variability of phytoplankton light absorption in canadian arctic seas. Journal of Geophysical Research 117 (C9), 1–17.

Claustre, H., Bricaud, A., Babin, M., Bruyant, F., 2002. Diel variations in *Prochlorococcus* optical properties. Limnology and Oceanography 47 (6), 1637–1647.

Coachman, L. K., 1986. Circulation, water masses, and fluxes on the southeastern bering sea shelf. Continental Shelf Research 5, 23–108.

Cosper, E., 1982. Influence of light intensity on diel variations in rates of growth, respiration and organic release of a marine diatom: comparison of diurnally constant and fluctuating light. Journal of Plankton Research 4 (3), 705–724.

Cross, J. N., Mathis, J. T., Bates, N. R., 2012. Hydrographic controls on net community production and total organic carbon distributions in the eastern bering sea. Deep-Sea Research II 65-70 (C), 98–109.

Cullen, J. J., 1990. On models of growth and photosynthesis in phytoplankton. Deep-Sea Research 37 (4), 667–683.

Diehl, S., Berger, S., Ptacnik, R., Wild, A., 2002. Phytoplankton, light, and nutrients in a gradient of mixing depths: field experiments. Ecology 83 (2), 399–411.

638 Dubinsky, Z., Stambler, N., 2009. Photoacclimation processes in phytoplankton:
639 mechanisms, consequences, and applications. Aquatic Microbial Ecology 56,
640 163–176.

641 Eisner, L. B., Gann, J. C., Ladd, C., Ciecciel, K., Mordy, C. W., 2016. Late
642 summer/early fall phytoplankton biomass (chlorophyll a) in the eastern bering
643 sea: spatial and temporal variations and factors affecting chlorophyll a con-
644 centrations. Deep-Sea Research II 134, 100–114.

645 Falkowski, P. G., Raven, J. A., 2007. Aquatic Photosynthesis, 2nd Edition.
646 Princeton University Press.

647 Fujiki, T., Taguchi, S., 2002. Variability in chlorophyll *a* specific absorption
648 coefficient in marine phytoplankton as a function of cell size and irradiance.
649 Journal of Plankton Research 24 (9), 859–874.

650 Gibson, C. E., 1985. Growth rate, maintenance energy and pigmentation of
651 planktonic cyanophyta during one-hour light:dark cycles. British Phycological
652 Journal 20 (2), 155–161.

653 Gray, R. W., 1931. The colour of the greenland sea and the migrations of the
654 greenland whale and narwhal. The Geographical Journal 78, 284–290.

655 Huisman, J., Sharples, J., Stroom, J. M., Visser, P. M., Kardinaal, W. E. A.,
656 Verspagen, J. M. H., Sommeije, B., 2004. Changes in turbulent mixing shift
657 competition for light between phytoplankton species. Ecology 85 (1), 2960–
658 2960.

659 Ikeya, T., Kashino, Y., Kudoh, S., Imura, S., Watanabe, K., Fukuchi, M., 2000.
660 Acclimation of photosynthetic properties in psychrophilic diatom isolates un-
661 der different light intensities. Polar Bioscience 13, 43–54.

662 Ji, R., Ashjian, C. J., Campbell, R. G., Chen, C., Gao, G., Davis, C. S., Cowles,
663 G. W., Beardsley, R. C., 2012. Life history and biogeography of calanus cope-
664 pods in the arctic ocean: an individual-based modeling study. Progress in
665 Oceanography 40–56 (1), 96.

Jochem, F. J., 1999. Dark survival strategies in marine phytoplankton assessed by cytometric measurement of metabolic activity with fluorescein diacetate. Marine Biology 135, 721–728.

Kauko, H. M., Taskjelle, T., Assmy, P., Pavlov, A. K., Mundy, C. J., Duarte, P., Fernández-Méndez, M., et al., L. M. O., 2017. Windows in arctic sea ice: Light transmission and ice algae in a refrozen lead. Journal of Geophysical Research: Biogeosciences 122 (6), 1486–1505.

Langdon, C., 1988. On the causes of interspecific differences in the growth-irradiance relationship for phytoplankton. ii. a general review. Journal of Plankton Research 10 (6), 1291–1312.

Lichtman, E., 2000. Growth rates of phytoplankton under fluctuating light. Freshwater Biology 44, 223–235.

Lomas, M. W., Moran, S. B., Casey, J. R., Bell, D. W., Tiahlo, M., Whitefield, J., Kelly, R. P., Mathis, J. T., Cokelet, E. D., 2012. Spatial and seasonal variability of primary production on the eastern bering sea shelf. Deep-Sea Research II 65–70, 126–140.

Long, M. C., 2010. Upper ocean physical and ecological dynamics in the ross sea, antarctica. Ph.D. thesis, Stanford University.

Marra, J., 1978. Phytoplankton photosynthetic response to vertical movement in mixed layer. Marine Biology 46, 203–208.

Matsuoka, A., Hill, V., Yannick, H., Babin, M., A Bricaud, A., 2011. Seasonal variability in the light absorption parameters of western arctic waters: Parameterization of the individual components of absorption for ocean color applications. Journal of Geophysical Research: Oceans 116.

Matsuoka, A., Larouche, P., Poulin, M., Vincent, W., Hattori, H., 2009. Phytoplankton community adaptation to changing light levels in the southern beaufort sea, canadian arctic. Estuarine, Coastal and Shelf Science 82, 537–546.

694 Moore, C. M., Suggett, D. J., Hickman, A. E., Kim, Y., Tweddle, J. F., Sharples,
695 J., Geider, R. J., Holligan, P. M., 2006. Phytoplankton photoacclimation
696 and photoadaptation in response to environmental gradients in a sea shelf.
697 Limnology and Oceanography 51 (2), 936–949.

698 Mordy, C. W., Stabeno, P. J., Cokelet, E. D., Ladd, C., Menzia, F. A., Proctor,
699 P., Wisegarver, E., 2012. Net community producn on the middle shelf of the
700 eastern bering sea. Deep-Sea Research II 65–70, 110–125.

701 Morgan-Kiss, R. M., Lizotte, M. P., Kong, W., Priscu, J. C., 2016. Photoad-
702 aptation to the polar night by phytoplankton in a permanently ice-covered
703 antarctic lake. Limnology and Oceanography 61, 3–13.

704 Nicklisch, A., 1998. Growth and light absorption of some planktonic cyanobac-
705 teria, diatoms, and chlorophyceae under simulated natural light fluctuations.
706 Journal of Plankton Research 20 (1), 105–119.

707 Palmer, M., Arrigo, K. R., Mundy, C. J., Ehn, J. K., Gosselin, M., Barber, D. G.,
708 Martin, J., Alou, E., Roy, S., Tremblay, J.-E., 2011. Spatial and temporal
709 variation of photosynthetic parameters in natural phytoplankton assemblages
710 in the beaufort sea, canadian arctic. Polar Biology 34, 1915–1928.

711 Palmer, M. A., van Dijken, G. L., Mitchell, B. G., Seegers, B. J., Lowry, K. E.,
712 Mills, M. M., Arrigo, K. R., 2013. Light and nutrient control of photosynthesis
713 in natural phytoplankton populations from the chukchi and beaufort seas,
714 arctic ocean. Limnology and Oceanography 58 (6), 2185–2205.

715 Peters, E., 1996. Prolonged darkness and diatom mortality ii: Marine temperate
716 species. Journal of Experimental Marine Biology and Ecology 207, 43–57.

717 Peters, E., Thomas, D. N., 1996. Prolonged darkness and diatom mortality
718 i: Marine antarctic species. Journal of Experimental Marine Biology and
719 Ecology 207, 25–41.

Platt, T., Harrison, W. G., Irwin, B., Horne, E. P., 1982. Photosynthesis and photoadaptation of marine phytoplankton in the arctic. Deep Sea Research 29 (10A), 1159–1170.

Platt, T., Jassby, A. D., 1976. The relationship between photosynthesis and light for natural assemblages of coastal marine phytoplankton. Journal of Phycology 12, 421–430.

Quigg, A., Beardall, J., 2003. Protein turnover in relation to maintenance metabolism at low photon flux in two marine microalgae. Plant, Cell and Environment 26, 693–703.

Rochet, M., Legendre, L., Demers, S., 1986. Photosynthetic and pigment responses of sea-ice microalgae to changes in light intensity and quality. Journal of Experimental Marine Biology and Ecology 101, 211–226.

Sakshaug, E., Slagstad, D., 1991. Light and productivity of phytoplankton in polar marine ecosystems: a physiological view. Polar Research 10 (1), 69–86.

Sambrotto, R. N., 2001. Nitrogen production in the northern arabian sea during the spring intermonsoon and southwest monsoon seasons. Deep-Sea Research II 48, 1173–1198.

Sambrotto, R. N., Burdloff, D., McKee, K., 2015. Spatial and year-to-year patterns in new and primary productivity in sea ice melt regions of the eastern bering sea. Deep-Sea Research II.

Sambrotto, R. N., Burdloff, D., McKee, K., 2016. Spatial and year-to-year patterns in new and primary productivity in sea ice melt regions of the eastern bering sea. Deep-Sea Research II 134, 86–99.

Sambrotto, R. N., Mordy, C., Zeeman, S. I., Stabeno, P. J., Macklin, S. A., 2008. Physical forcing and nutrient conditions associated with patterns of chl a and phytoplankton productivity in the southeastern bering sea during summer. Deep-Sea Research II 55, 1745–1760.

747 Sambrotto, R. N., Niebauer, H. J., Goering, J. J., Iverson, R. L., 1986. Rela-
748 tionships among vertical mixing, nitrate uptake, and phytoplankton growth
749 during the spring bloom in the southeast bering sea middle shelf. Continental
750 Shelf Research 5 (1/2), 161–198.

751 Sherr, E. B., Sherr, B. F., Ross, C., 2013. Microzooplankton gazing impact
752 in the bering sea during spring sea ice conditions. Deep Sea Research II 94,
753 57–67.

754 Smith Jr., W. O., Donaldson, K., 2015. Photosynthesis-irradiance responses in
755 the ross sea, antarctica: a meta-analysis. Biogeosciences 12 (11), 3567–3577.

756 Stabeno, P. J., Danielson, S. L., Kachel, D. G., Kachel, N. B., Mordy, C. W.,
757 2016. Currents and transport on the eastern bering sea shelf: An integra-
758 tion of over 20 years of data. Deep Sea Research Part II: Topical Studies in
759 Oceanography 134, 13–29.

760 Stabeno, P. J., Farley, Jr, E. V., Kachel, N. B., Moore, S., Mordy, C. W., Napp,
761 J. M., Overland, J. E., Pinchuk, A. I., Sigler, M. F., 2012. A comparison of
762 the physics of the northern and southern shelvesof the eastern bering sea in
763 summer. Deep Sea Research II 65–70, 14–30.

764 Stoecker, D. K., Weigel, A., Goes, J. I., 2013. Microzooplankton grazing in the
765 eastern bering sea in summer. Deep Sea Res. II 109, 145–156.

766 Strzepek, R. F., Harrison, P. J., 2004. Photosynthetic architecture differs in
767 coastal and oceanic diatoms. Nature Letters 431 (7 Oct), 689–692.

768 Sverdrup, H. U., 1953. On the conditions for the vernal blooming of phyto-
769 plankton. Journal du Conseil International pour l'Exploration de la Mer 18,
770 287–295.

771 van Hilst, C. M., Smith, Jr, W. O., 2002. Photosynthesis/irradiance relation-
772 ships in the ross sea, antarctica and their control by phytoplankton assemblage
773 composition and environmental factors. Marine Ecology Progress Series 226,
774 1–12.

775 Varpe, Ø., Jørgensen, C., Tarling, G. A., Fiksen, Ø., 2007. Early is better:
776 seasonal egg fitness and timing of reproduction in a zooplankton life-history
777 model. Oikos 116, 1331–1342.

778 Wu, Z., Song, L., Li, R., 2008. Different tolerances and responses to low temper-
779 ature and darkness between waterbloom forming cyanobacterium *Microcystis*
780 and a green alga *Scenedesmus*. Hydrobiologia 596, 47–55.

781 Wulff, A., Roleda, M. Y., Zacher, K., Wiencke, C., 2008. Exposure to sudden
782 light burst after prolonged darkness– a case study on benthic diatoms in
783 antarctica. Diatom Research 23 (2), 519–532.

784 Zhang, J., Woodgate, R., Moritz, R., 2010. Sea ice response to atmospheric and
785 oceanic forcing in the bering sea. Journal of Physical Oceanography 40 (8),
786 1729–1247.

Parameter		Best Fit Range	Units
Max P growth rate (Summer)	$\mu_{0,sum}$	2.6 – 3.6	d^{-1}
Max P growth rate (Winter)	$\mu_{0,win}$	0.2 – 0.4	
Initial growth-light slope (Sum)	α_{sum}	0.10 – 0.14	$(W\ m^{-2})^{-1}\ d^{-1}$
Initial growth-light slope (Win)	α_{win}	0.008 – 0.012	
Compensation intensity	E_C	13 – 17	$W\ m^{-2}$
Max ingestion rate	I_0	1.1 – 1.9	d^{-1}
Phytoplankton mortality	m_P	0.01 – 0.03	d^{-1}
Phyto loss via aggregation	m_{aggr}	0.005 – 0.015	$(\mu M\ N)^{-1}\ d^{-1}$
Light attenuation, sea-water	att_{sw}	0.05 – 0.07	m^{-1}
Light attenuation, phytoplankton	att_P	0.002 – 0.009	$m^{-1}\ \mu M\ N^{-1}$

Table 3: Parameters varied and the ranges of values providing the best fits to observation data. Without seasonality, μ_0 and α were constant.

Variable	Time Period	Mean Obs. Value
NO_3, top 35 metre average [μM N]	10–11 Apr (pre-bloom)	16.5
	26–30 Apr (early bloom)	7.7
	6–7 May (late bloom)	1.9
	26 June – 6 July (summer)	4.3
Integrated phytoplankton P [g C m^{-2}]	10–11 Apr	0.86
	26–30 Apr	34
	6–7 May	47
	26 June – 6 July	2.0
Integrated microzooplankton Z [g C m^{-2}]	10–11 Apr	0.0028
	26–30 Apr	0.066
	6–7 May	0.18
Phytoplankton specific growth rate μ [day^{-1}]	10–11 Apr	0.091
	26–30 Apr	0.38
	6–7 May	0.19
	26 June – 6 July	0.22
Specific grazing rate I [day^{-1}]	10–11 Apr	0
	26–30 Apr	0.15
	6–7 May	0.17
	26 June – 6 July	0.24
f-ratio	26–30 Apr	0.94
	6–7 May	0.71
	26 Jun – 6 July	0.31

Table 4: Target values for model runs from IEB60 data, spring to summer 2009 (Mordy et al., 2012; Lomas et al., 2012; Cross et al., 2012; Sherr et al., 2013; Stoecker et al., 2013; Sambrotto et al., 2016).